Numerical Simulation and Visualization of a Flowfield by Interaction of Two Parallel Two-Dimensional Freejets

By

Koji TESHIMA* and Hiroyuki NAKATSUJI*

(February 5, 1987)

Summary: Flowfields resulted from interaction of two equivalent freejets issued from two parallel two-dimensional sonic nozzles at various nozzle distances and at various values of the stagnation to ambient pressure ratio are investigated numerically and by visualization. A strong shear flow region appears between the two jets, which is observed by visualization, is simulated well by the present calculation. Agreements of the parameters representing the whole structure of the flowfield, such as the location of the interaction point of the inner lateral shock with the outer one, the location of the shock reflection point on the symmetry plane and the deflection angle of each jet by interaction, are very well between the simulation and the experiment so far nearly two-dimensional flows are realized in the experiment.

1. INTRODUCTION

Flowfields resulted from interaction of several supersonic jets are of importance for estimation of the base pressure and temperature of a multi-booster rocket as well as for understanding of the whole jet structure and the whole jet size relating to the jet interaction with bodies. Several experiments have been made for the interaction flowfield of two axisymmetric freejets [1, 2], but an accurate numerical simulation of such a three-dimensional flowfield is still difficult except a limited flow region [3] because of a practically available capacity of a computer. To approach the problem it is easy to start with a two-dimensional flowfield.

In the presnt study a flowfield produced by interaction of two equivalent freejets issued from two parallel two-dimensional sonic nozzles is investigated numerically and by visualization. The nozzle distance, W, and the pressure ratio (the stagnation to the chamber pressure, p_0/p_∞) were changed in order to examine the effect of interaction on the whole jet structure. In the numerical simulation the PLM scheme, which has been shown to be useful for supersonic flows with discontinuities such as shocks and contact surfaces in the preceding reports [4–6], was used. The visualization was made by laser induced fluorescence of iodine molecules seeded in the flow medium [7], which has become a well established one. The present study is also an extension of the preceding study of a two-dimensional freejet [4].

* Department of Aeronautical Engineering, Kyoto University.
** Tanegashima Space Center, National Space Development Agency of Japan.

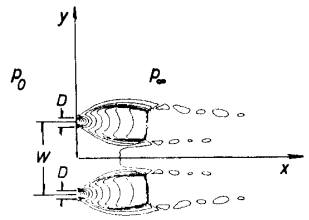

Fig. 1. Flowfield by interaction of two parallel two-dimensional freejets.

2. Numerical Method

We consider a flowfield shown in Fig. 1, where two equivalent freejets are issued from two identical two-dimensional sonic nozzles separated by a certain distance with their centers parallel each other. The flow is two-dimensional and the coordinates system is taken so as the y-axis to be along the nozzle exit and the x-axis to be perpendicular to it. The origin is taken to be the center of the two nozzles. The ambient pressure is finite and is kept constant so as the pressure ratio of the stagnation to the ambient becomes constant. Continuum gasdynamics without heat conduction and friction is used to describe the flowfield, then the conservation equations of mass, momentum and energy for the flow in a conservation form can be written as

$$\frac{\partial U}{\partial t}+\frac{\partial F}{\partial x}+\frac{\partial G}{\partial y}=0. \tag{1}$$

where,

$$U=\begin{bmatrix}\rho\\ \rho u\\ \rho v\\ \rho E\end{bmatrix},\qquad F=\begin{bmatrix}\rho u\\ \rho u^2\\ \rho uv\\ \rho u(E+p/\rho)\end{bmatrix},\qquad G=\begin{bmatrix}\rho v\\ \rho uv\\ \rho v^2+p\\ \rho v(E+p/\rho)\end{bmatrix}. \tag{2}$$

In these equations, t is time, u and v are the flow velocity components in x and y directions, respectively, ρ, p are the density and pressure, and E the energy per unit mass given by

$$E=\frac{p/\rho}{(\gamma-1)}+\frac{1}{2}(u^2+v^2), \tag{3}$$

for a perfect gas with specific heat ratio γ. Here, the properties have been nondimensionalized using the following reference values; the stagnation values (suffix 0) for pressure and density, $a_0/\sqrt{\gamma}$ (a_0: speed of sound at the stagnation) for velocities, nozzle width, D, for distances and $D\sqrt{\gamma}/a_0$ for time.

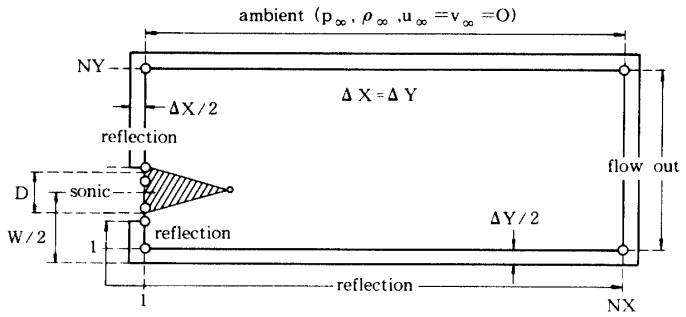

Fig. 2. Computational region, boundary conditions, and initial condition.

Table 1. Flow conditions and mesh size for calculated cases

P_0/P_∞	W/D (D=4)			
	3	6	9	12
10	150× 40			
20	200× 40	200× 40	200×50	200×50
30	300× 60	240× 60	240×60	
40	400× 80	320× 80		
50	400×100	400×100		

The governing equations were solved by a finite difference method. By using the operator splitting method each system of hyperbolic conservation laws in one-dimension was solved by a scheme so called Piecewise Linear Method (PLM). This scheme has been used to simulate supersonic jets from sonic orifices [4, 5] and from a hypersonic nozzle [6] and has been proved to provide good simulation of flowfields by comparing the results with their flow visualization. In the scheme the numerical fluxes are computed by solving zone interface Riemann problems whose time-centered left and right states are computed from the characteristic form of the equations. The details can be seen in ref. 5.

The computational region, which is the upper half of the flowfield, the boundary conditions and the initial conditions are illustrated in Fig. 2. The mesh size depends on the flow condition and is listed in Table 1. From a restriction of the allocable memory region of the computer, four grid points were assigned to the nozzle width, D, for most of the cases.

Sonic conditions were applied to the nozzle exit while mirror reflections were assumed on the solid wall of the left boundary. At the circumference, namely at the top of Fig. 2, the ambient conditions of the expansion chamber were used as the boundary conditions. The conditions of zero-gradients of the flow parameters, flow-out conditions, were used at the right-hand side of the calculation region.

Sonic conditions were distributed initially over the shaded region in Fig. 2. The ambient conditions were given to the rest of the grid points as the initial conditions. The time increment Δt was determined at each step considering the CFL condition. In order to obtain a faster convergence the following modifications of the preceding

scheme were made;
1) in order to reduce the influence of the out-flow boundary condition and to reduce the total number of mesh the grid interval was increased gradually up to 4 times of the normal one ($\Delta X=\Delta Y=0.2$) in the region downstream of an expected location of the shock reflection on the symmetry plane.
2) We added a restriction that the x-component of the flow velocity must be always positive except in the region surrounded by two inner jet boundaries and the wall.
With these modifications an almost converged solution was obtained in the most parts of the flowfield after 2000–3000 time steps depending on the flow condition. We note that at least for the region upstream of the shock reflection on the symmetry plane an almost steady flowfield has been obtained even before 2000 time steps.

The calculation was made on a vector-computer, FACOM VP-200 at the Digital Processing Center of Kyoto University. It took about 0.5 sec per time step for the largest mesh size case.

3. Numerical Results

The calculated results are shown in Figs. 3–7. Density contour lines of the flowfields for different nozzle distances at various values of the pressure ratio, are shown in Fig. 3. Changes of flow properties along the symmetry plane (strictly, along the nearest grid points to it) for various nozzle distances at a fixed pressure ratio are shown in Fig. 4. In Fig. 5 it shows changes of the flow properties along the symmetry plane and the nozzle-center plane (again along the nearest grids to it) for two different nozzle distances, W/D=6 and 3, at various values of the pressure ratio. Flow property changes in y-direction at various distances from the nozzle exit are shown in Fig. 6 for W/D=9 and $p_0/p_\infty=20$, and for W/D=3 and $p_0/p_\infty=20$. In Fig. 7 equi-Mach lines for the supersonic flow region are drawn for the case of W/D=9 and $p_0/p_\infty=20$.

4. Visualization by Laser Induced Fluorescence

Although it is almost impossible to realize a complete two-dimensional supersonic jet, a nearly two-dimensional flow can be obtained for low pressure ratios by use of a slit nozzle with a large aspect ratio as shown in the previous studies [8–10]. In the present study the slit width, D, was 0.4 mm and the slit length, L, was 18 mm (aspect ratio L/D=45). The distance of the centers of the two slits was changed from 3 to 12 slit widths corresponding to the numerical simulation. Room temperature nitrogen gas at a stagnation pressure of 100 Torr was used. The pressure ratio was changed also correspondingly to the numerical simulation. From Fig. 3 of our preceding paper [10], the normal shock location changes linearly with the pressure ratio, as is expected by the two-dimensional theory, up to about 60 for jets issued from a slit nozzle with aspect ratio 51. Therefore, we considered that the flow was nearly two-dimensional in the most cases of the present experiment. Flow visualization was made using the laser induced fluorescence method, the details of which is described in ref. 7.

Visualized flowfields are shown in Fig. 8 for different values of the pressure ratio at

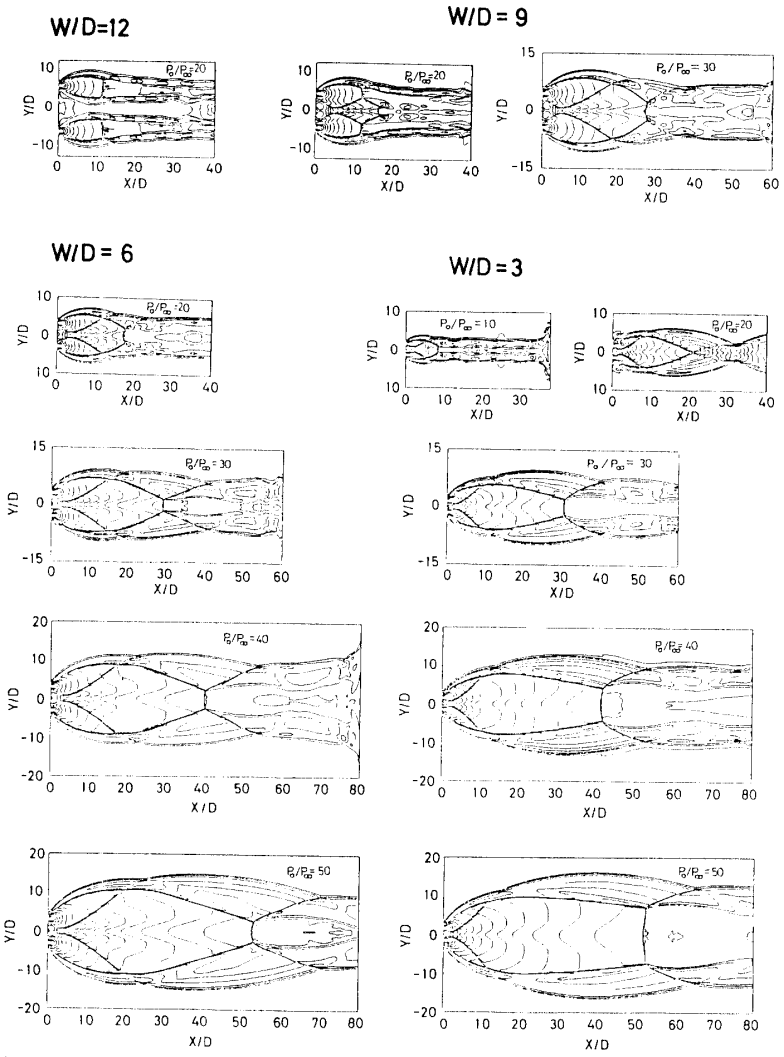

Fig. 3. Density contour lines of flowfields for different nozzle distances at various values of pressure ratio.

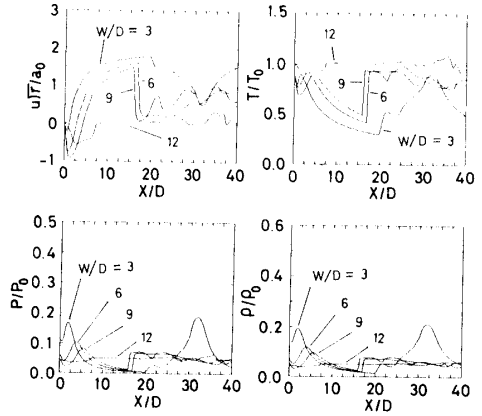

Fig. 4. Calculated flow properties on symmetry plane for different nozzle distance at $p_0/p_\infty=20$.

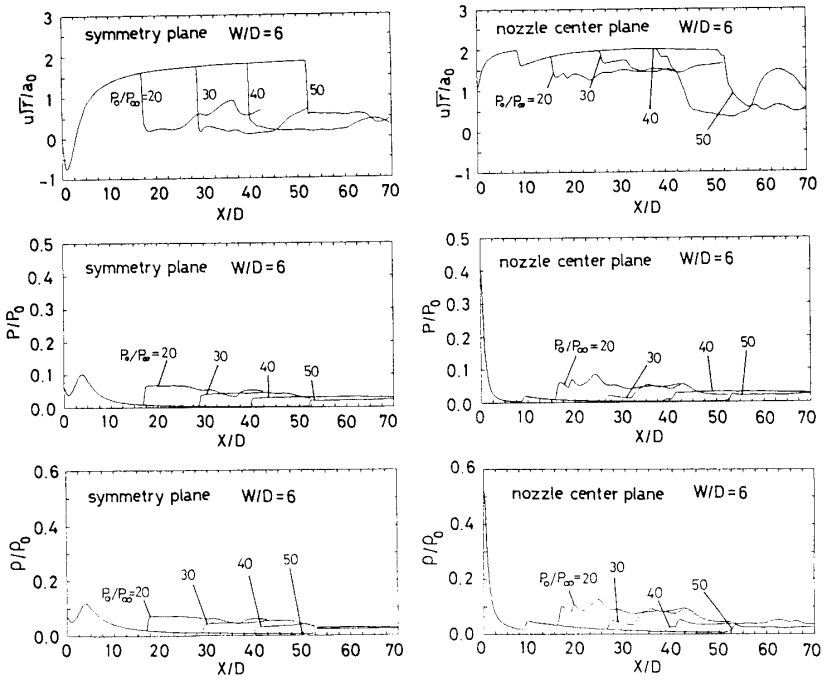

(a)

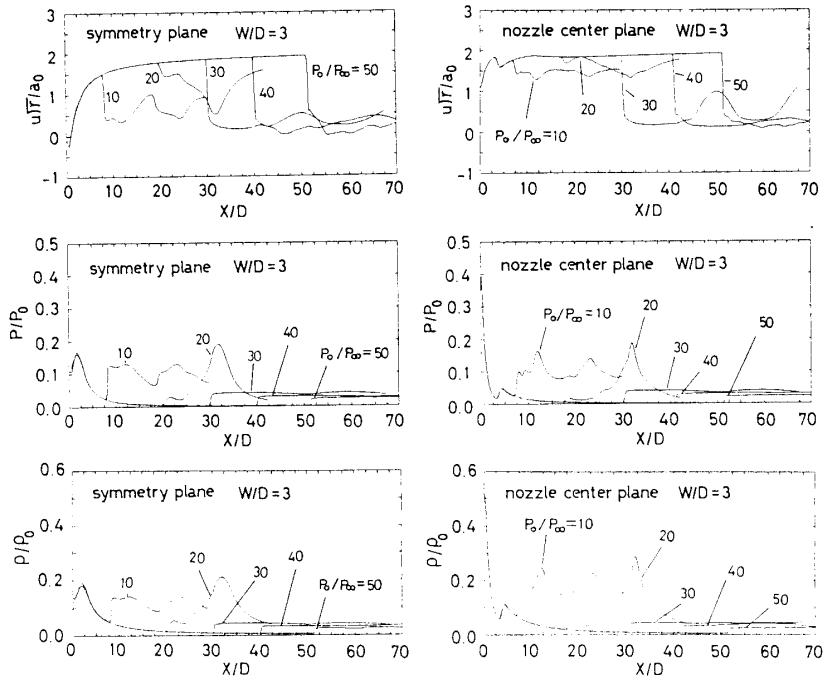

(b)

Fig. 5. Calculated flow properties on the symmetry plane and on the nozzle center plane. (a) W/D=6 and p_0/p_∞=20~50, (b) W/D=3 and p_0/p_∞=10~50.

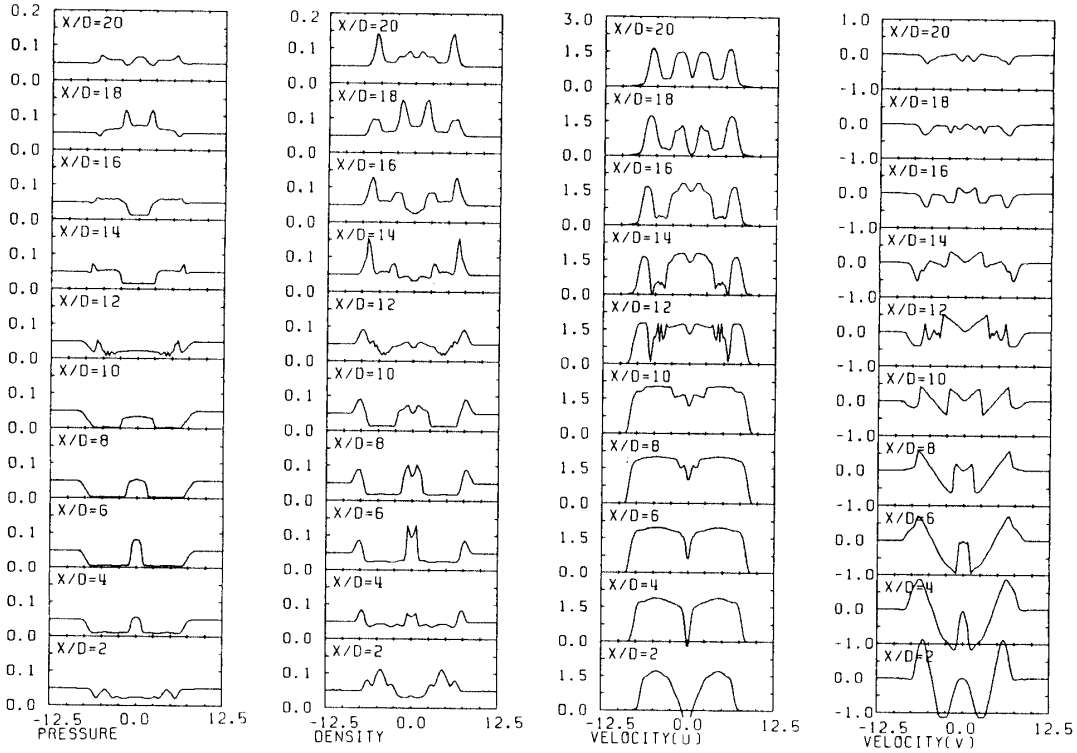

Fig. 6. Changes of flow properties in y-axis at various distances from nozzle exit. (a) W/D=9, $p_0/p_\infty=20$ and (b) W/D=3 and $p_0/p_\infty=20$.

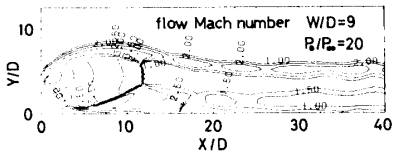

Fig. 7. Equi-Mach number lines in supersonic flow region for case of W/D=9 and $p_0/p_\infty=20$.

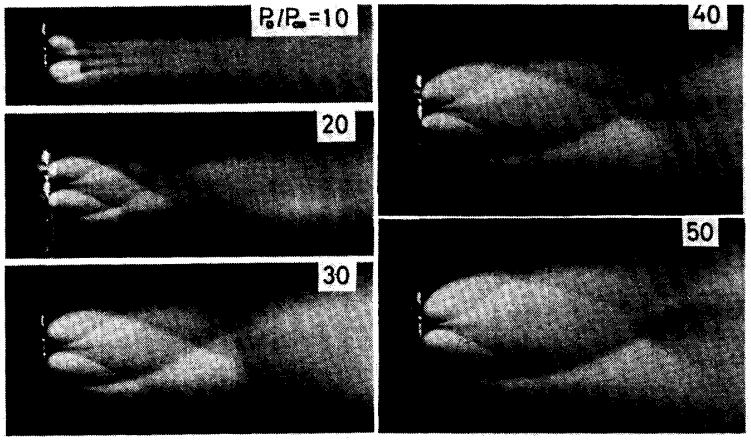

Fig. 8. Visualized flowfields by laser induced fluorescence. W/D=6 (D=0.3 mm, aspect ratio 45) and $p_0/p_\infty=10\sim50$.

a fixed nozzle distance, W/D=6. The unsymmetry of the flowfield was caused by slight difference in the width in two slits, which was not larger than 10%.

5. Discussions

At the largest nozzle distance, (Fig. 3, W/D=12), interaction between the two jets is weak and each jet structure does not seem to be changed except deformed inner jet boundaries and slight inclination of each jet center toward the symmetry plane. A very weak interaction flowfield appears between the two jets. Decreasing the distance (W/D=9) keeping the pressure ratio constant ($p_0/p_\infty=20$), the inner lateral shock and the jet boundary interact with each other and produce a strong interaction flowfield along the symmetry plane. Each jet still forms a normal shock on its center plane. The inner reflected shock at the normal shock is stronger than the outer one and makes Mach reflection on the symmetry plane. The outer half of the jet is not influenced by the interaction until the normal shock, after that the flow seems to shrink due to lower pressure of the inner flowfield. With a further decreasing of the nozzle distance (W/D=6) keeping the same pressure ratio or increasing the pressure ratio ($p_0/p_\infty=30$) at the same nozzle distance, the inner lateral shock interact with outer one directly without forming a normal shock. This is a typical flowfield produced by the two interacting jets in the present study and its structure is illustrated in Fig. 9. The inner reflected shock becomes more stronger than the outer one, forms an outer shock for the secondary jet produced by the interaction, and reflects on the symmetry plane as Mach reflection.

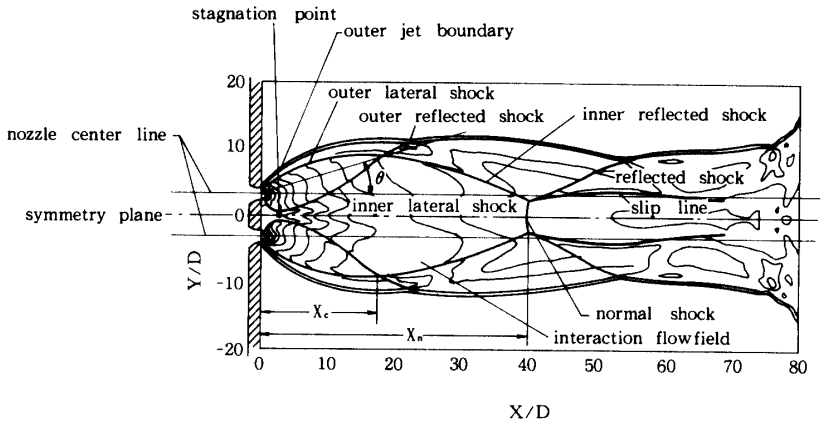

Fig. 9. Structure of flowfield by interaction of two parallel two-dimensional freejets.

For $p_0/p_\infty=20$ and W/D=3 (Fig. 3) the inner reflected shock forms a normal reflection on the symmetry plane and then the flow remains still supersonic after the shock reflection. This is the only case of the normal reflection among the presently calculated cases. This normal reflection was observed by visualization not only for the corresponding flow condition but also at smaller values of the pressure ratio than 30 for nozzle distances, W/D=3 and 6, as can be seen from Fig. 8. The transition of the shock reflection from normal to Mach seems to be very sensitive to the nozzle Reynolds number for the present flow condition and will be studied further in an extended research. The jet width becomes narrow downstream of the shock reflection, where the jet boundary intersect with the reflected shock. This flow pattern is similar to that of an underexpanded jet from a narrow angle conical nozzle [6]. The interaction flowfield becomes a large portion of the whole flowfield as increasing the pressure ratio and occupies almost the main jet core.

For a fixed nozzle distance the flow properties along the symmetry plane are the same for different pressure ratios until the inner reflected shock reflects on the symmetry plane, and those on the nozzle center plane are the same until the inner lateral shock intersects as can be seen in Fig. 5. This indicates that the convergence of the calculation has been obtained at least up to the shock reflection point on the symmetry plane.

In the interaction flowfield surrounded by the two inner lateral shocks a stagnation point exists on the symmetry plane as can be seen from the velocity change along the symmetry plane (Fig. 5) and the velocity distribution in y-direction (Fig. 6). For a fixed value of the pressure ratio the stagnation point moves downstream with increasing the nozzle distance, i.e. weaker interaction, as can be seen from Fig. 4. The pressure and density at the stagnation point become larger than the ambient values and they increase with decreasing the nozzle distance, i.e. stronger interaction. For a fixed nozzle distance, however, the location of the stagnation point and the flow properties on it are the same and hence the interaction flowfield surrounded by the two nozzle center planes and the wall is identical up to the shock reflection point on the symmetry plane for different values of the pressure ratio. Since changes of flow properties in y-direction near the symmetry plane are large and since we calculated

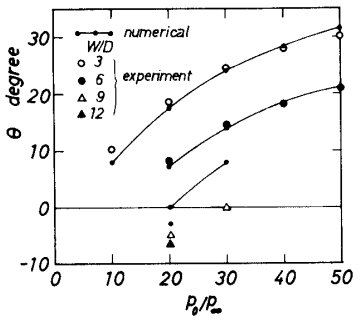

Fig. 10. Comparison of deflection angle of each jet between simulation and experiment for various flow conditions.

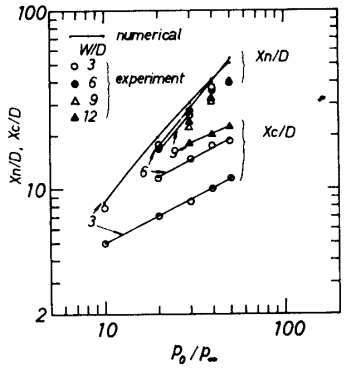

Fig. 11. Comparison of location of interaction point of inner lateral shock with outer one, X_c, and that of reflection point of inner reflected shock on symmetry plane, X_n, between the simulation and the experiment.

them on the grid points separated a half-grid size from the symmetry plane, their peak values appeared at u=0, shown in Fig. 4 and 5, will be less than the true stagnation values. Actually, the temperature at stagnation calculated from these values is somewhat less than the nozzle source temperature. However, it was confirmed that the temperature at the stagnation point approaches to the source value and the pressure and the density also increase to certain values by decreasing the grid separation.

The flow is accelerated to a supersonic flow and makes a strong shear flow region with the flow which enters into this region through the inner lateral shocks. The Mach line in this region can be seen in Fig. 7. The density gradient in y- direction near the symmetry plane is large while that of pressure is smooth, then the temperature gradient is also large. That is, the density is lower and the temperature is higher along the symmetry plane than its outer flow region. Therefore, this shear flow region can be clearly seen by visualization as is shown in Fig. 8, because the intensity of laser induced fluorescence depends strongly on gas temperature and density [7].

With increasing the pressure ratio and/or decreasing the nozzle distance, interaction between the inner and outer lateral shocks becomes stronger and each jet is directed outward, i.e. the deflection angle, θ, defined in Fig. 9 becomes larger. Therefore, the interaction flowfield downstream of the stagnation becomes wider and spreads more, and then the strong shear flow region is eased, i.e. the density gradient in y-direction becomes small. The deflection angle is plotted against the pressure ratio for different nozzle distances in Fig. 10. For W/D=3 and 6 the deflection angles obtained from numerical simulation and visualization agree very well, but for larger nozzle distances the observed angle is smaller than that by the simulation. This may be attributed to the three-dimensionality of the jet in the experiment. Since the two-dimensional nature will be lost more in the outer flow region of a jet issued from a slit with a finite aspect ratio, then for a larger nozzle distance the interaction between these outer

flows occurs less two-dimensionally and will be weaker than the two-dimensional theory.

The normal shock is concave to the flow direction since the flow velocity is slower and the density is lower inside the jet as is shown in Fig. 6. This is in contrast with the shape of the normal shock of a single undisturbed jet [4], which is convex due to the inverse distribution of flow velocity and density.

Typical parameters representing the size of the interacting jet may also include the locations of shock interaction; the interaction point of the inner lateral shock with the outer one, X_c and the shock reflection point of the inner reflected shock on the symmetry, X_n, as well as the jet deflection angle, as shown in Fig. 9. Comparisons of these values between the simulation and the experiment are shown in Fig. 11. For the values of X_c agreements between them are very good but for X_n the values obtained by visualization are smaller than those by the simulation and the difference becomes larger with increasing the pressure ratio. This is mainly due to the three-dimensional effect of the flow, which shortens the location of the normal shock in case of a single jet as is shown in our previous report [10]. Here, we note that the value of X_n increases linearly with the pressure ratio and is larger than the location of the normal shock for a single two-dimensional jet at the same pressure ratio. That is, as a result of interaction the whole jet becomes longer. On the other hand the value of X_c increases with pressure ratio as $(p_0/p_\infty)^{0.5}$.

6. Conclusions

The whole structure of a flowfield resulted by interaction of two parallel two-dimensional freejets was made clear by the numerical simulation and by visualization in the following subjects.

1) Values of parameters representing the whole jet structure, such as the location of the interaction point of the inner lateral shock with the outer one, the location of the shock reflection point on the symmetry plane, and the deflection angle of each jet were determined. Agreement between the simulation and the experiment was very well so far a nearly two-dimensional flow was realized in the experiment.

2) A strong shear flow region was simulated and its existence was comfirmed by flow visualization.

3) There is a stagnation point in the interaction region, where the pressure and density are larger than the ambient values and the temperature is expected to become the nozzle source value. The location of the stagnation point depends on the nozzle distance not on the pressure ratio.

4) Upstream of the stagnation point there is a region where the pressure is larger than the ambient and the temperature is close to the stagnation value. However, an accurate estimation of these values must be made with a finer grid interval.

Acknowledgements

The numerical simulation of the present study was performed under the Program

Development Projects of the Data Processing Center of Kyoto University.

REFERENCES

[1] Soga, T., Takanishi, M. and Yasuhara, M.: "Experimental Study of Interaction of Underexpanded Free Jets", Rarefied Gas Dynamics, Oguchi, H. ed., (Tokyo Univ. Press, Tokyo, 1984), Vol. II pp. 743–749

[2] Dankert, C.: "Flow in the Interaction Region of Two Parallel Free Jets", Rarefied Gas Dynamics, Boffi, V. and Cercignani, C. ed., (B. G. Teubner, Stuttgart, 1986) Vol. II, pp. 486–494.

[3] D'Attorre, L. and Yoshihara, H.: "Problem of Rocket Exhaust Plume Interactions", Proceedings of the 7th International Symposium on Space Technology and Sciences, Tokyo, (Agne, Tokyo, 1967) p. 407.

[4] Teshima, K. and Nakatsuji, H.: "Numerical Simulation of Two-Dimensional Freejet Flow-Fields" ISAS Report SP. 4 (1986) pp. 89–95.

[5] Saito, T., Nakatsuji, H. and Teshima, K.: "Numerical Simulation and Visualization of Freejet Flow-Fields", Trans. Japan Soc. Aeron. and Space Sci., **28** (1986), pp. 240–247.

[6] Teshima, K., and Sommerfeld, M.: "Visualization and Numerical Simulation of Supersonic Microjets", (to be appeared in *Experiments in Fluids*)

[7] Teshima, K., Moriya, M. and Mori, T.: "Visualization of a Free Jet by a Laser Induced Fluorescence Method", J. Japan Soc. Aeron. and Space Sci. **32** (1984) pp. 61–64. (in Japanese): Teshima, K. and Nakatsuji, H.: "Visualization of Rarefied Gas Flows by a Laser Induced Fluorescence Method", Rarefied Gas Dynamics, Oguchi, H. ed., (University Tokyo Press, Tokyo, 1984), pp. 447–454.

[8] Beylich, A. E.: "Struktur von Uberschall-freistrahlen aus Schitzlenden", Z. Flugwiss. Weltraumforsch. **3** (1979), Heft 1, pp. 48–58.

[9] Dupeyrat, C.: "Two- and Three-Dimensional Aspects of a Freejet Issuing from a Long Rectangular Slit", Rarefied Gas Dynamics, Fisher, S. S. ed., (AIAA Press, New York, 1981), pp. 812–819.

[10] Teshima, K. and Nakatsuji, H.: "Structure of Freejets from Slit Orifices", Rarefied Gas Dynamics, Boffi, V. and Cercignani, C. ed., (B. G. Teubner, Stuttgart, 1986), Vol. II PP. 595–604.